

Control of chaos in conservative flows

Liu Zonghua

*CCAST (World Laboratory) P.O. Box 8730, Beijing, 100080, People's Republic of China;
Graduate School, China Academy of Engineering Physics, P.O. Box 8009, Beijing, 100088, People's Republic of China;
and Department of Physics, Guangxi University, Nanning, 530004, People's Republic of China*

Chen Shigang

*Institute of Applied Physics and Computational Mathematics, P.O. Box 8009, Beijing, 100088, People's Republic of China
(Received 2 December 1996; revised manuscript received 15 January 1997)*

The present paper discusses the control of chaos in conservative flow. Two methods are introduced, depending on whether the perturbations to the state are variables introduced on a proportional or an additive fashion. The maximum Lyapunov exponents of new creating periods are given. The method is robust against external noise. [S1063-651X(97)13406-7]

PACS number(s): 05.45.+b, 03.20.+i, 46.10.+z

I. INTRODUCTION

Nowadays, a number of methods have been proposed for control of chaos [1–10]. Pioneering is the Ott-Grebogi-Yorke (OGY) method [1]. Shortly afterwards many related methods were presented, such as the modified OGY methods [2,3], the occasional proportion feedback (OPF) or conventional linear feedback methods [4,5], the entrainment and migration control techniques [6,7], and our continuous parameter adjusting method [8,9], etc. The OGY and its modified methods convert chaotic motion into that of the congruous unstable periodic orbit by applying small, time-dependent perturbations to a system parameter. The OPF and conventional linear feedback methods are used to control a chaotic system with a trial and error feedback gain, and the system remains nonlinearity. The entrainment and migration control techniques transfer one attractor to another by a switching controller. Our method can direct nonlinear dynamic systems to any desired orbit. However, all these methods are designed for dissipative systems. For the Hamiltonian chaos, only the modified OGY method is found [10]. This method has a disadvantage in practical application, which needs to know details about the location of the target unstable periodic orbit. In this paper, we consider two kinds of periodic impulsive methods of controlling conservative flow. One applies additive perturbations on the system variables and the other applies multiplicative perturbation on the system variables. These methods, which are not necessary to know more details of the system, are used successfully in dissipative systems [11–13].

Sprott [14] made a systematic examination of general three-dimensional autonomous ordinary differential equations with quadratic nonlinearities, and uncovered 19 distinct simple examples of chaotic flows, with either five terms and two nonlinearities, or six terms and one nonlinearity. Only case *A* is a volume-conserving system and the others are dissipative systems with strange attractors. In this contribution, we use case *A* as an example to illustrate how the periodic impulsive method works.

The present paper is organized as follows. In Sec. II, the additive impulsive methods are investigated and case *A* is

used as the test bed. The regions of the additive perturbations, in which period-1 and period-2 are controlled, are given. Moreover, the maximum Lyapunov exponent is calculated. In Sec. III, the multiplicative impulsive method is studied and some periodic windows are given. Finally, in Sec. IV the effects of different types of noise on the two methods are considered and the main conclusions are listed.

II. ADDITIVE IMPULSIVE METHOD

The trajectory of the conservative flow runs in phase space. We expect to find a proper Poincaré section so that the behavior of the system will be simplified on the section. Generally speaking, the points on the section will not be identity in the chaotic band. However, if a periodic pulse is given on the section, some points of the Poincaré section will become identity. In other words, we create a new periodic orbit. In the present method we add a perturbation to the system variables,

$$x'_i = x_i + \gamma_i \quad (1)$$

where x_i represents the i th variable of the system on the Poincaré section and γ_i , which can be positive or negative, regulates the strength of the pulse. One can think of a practical implementation of this idea in the case of a batch chemical reactor consisting of the injection of some amount of either an insert compound or one of the i components.

As an application, we use case *A* [14] as an example

$$\begin{aligned} \dot{x} &= y, \\ \dot{y} &= -x + yz, \\ \dot{z} &= 1 - y^2. \end{aligned} \quad (2)$$

Its time-reversal invariance is evident from the equations. Reference [14] pointed out that the three Lyapunov exponents are 0.014, 0, and -0.014 . It is well known that the sum of the three exponents is the average rate of fractional volume expansion along the trajectory. So case *A* is a volume-

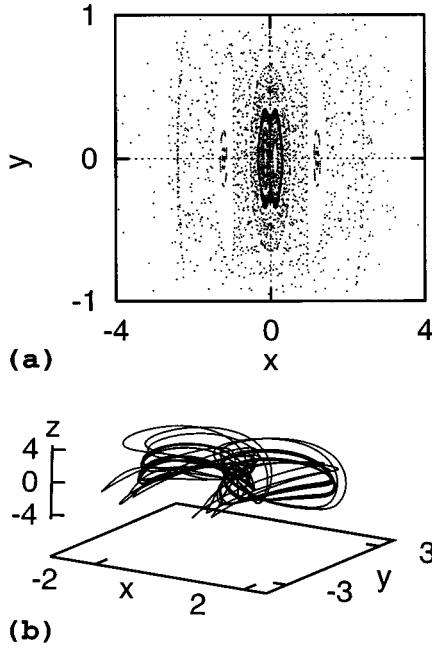


FIG. 1. (a) Poincaré section at $z=0$ for the conservative chaotic case A; (b) a trajectory in phase space for initial point $(0.0, 5.0, 0.0)$ when the transient process is discarded.

conserving system. In order to confirm this point, we calculate the divergence of the flow, which is the trace of the Jacobian matrix J

$$\frac{1}{V} \frac{dV}{dt} = \text{Tr}J = \frac{\partial \dot{x}}{\partial x} + \frac{\partial \dot{y}}{\partial y} + \frac{\partial \dot{z}}{\partial z} = \lambda_1 + \lambda_2 + \lambda_3 = z. \quad (3)$$

Obviously, the trace depends on the variable z . Choosing different initial points (except for the original point), and observing the evolution of variable z , we find that the variable z finally oscillates within a region surrounding zero and its average is zero. Hence, case A is a really conservative system. Figure 1(a) shows the Poincaré section of Eq. (2) in which points are plotted where the trajectory punctures the $z=0$ plane for various initial conditions. The quasiperiodic orbits are surrounded by a chaotic region. Figure 1(b) shows a trajectory in phase space for an initial point $(0.0, 5.0, 0.0)$ when the transient process is discarded. Throughout this paper we will always use $(0.0, 5.0, 0.0)$ as an initial point.

Adding periodic pulses to Eq. (2), we have

$$\begin{aligned} \dot{x} &= y + \gamma_1 \delta(z) \dot{z} \theta(\dot{z}), \\ \dot{y} &= -x + yz + \gamma_2 \delta(z) \dot{z} \theta(\dot{z}), \\ \dot{z} &= 1 - y^2, \end{aligned} \quad (4)$$

where $\delta(z)$ is Dirac's δ function, γ_1 and γ_2 regulate the intensity of periodic pulses, and $\theta(\dot{z})$ denotes the direction of crossing Poincaré section. In order to avoid two directions of crossing the plan $z=0$, we define the Poincaré section by that $z=0$ and $\dot{z}>0$. That is $\theta(\dot{z})=+1$ if $\dot{z}>0$ and $\theta(\dot{z})=0$ if $\dot{z}<0$. Restricting the intensity of periodic pulses γ_1 and γ_2 in the range -0.5 – 0.5 , we can find out the regions

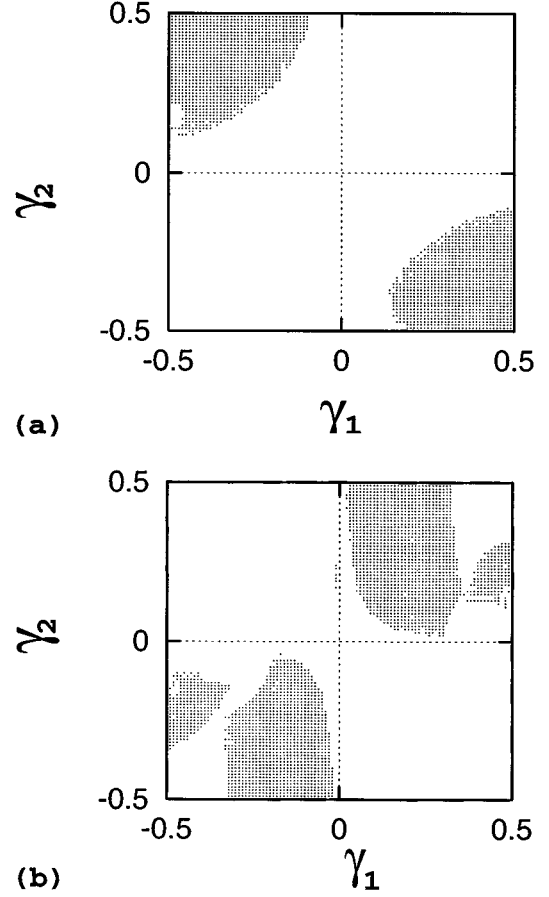


FIG. 2. The regions of period-1 and period-2 when γ_1 and γ_2 vary in range $-0.5 \sim 0.5$. (a) regions of period-1, (b) regions of period-2.

in which the period- n exists. For finding the regions of period- n , we let the $(n+1)$ th point of the Poincaré section identify with the first point. The set of equations (4) has been integrated by using a stable fixed-step fourth-order Runge-Kutta method with a step size of $\Delta t=0.01$ time units. The maximum allowable error is 10^{-6} . Figure 2 shows the results where the shadows in (a) denote the regions of period-1 and the shadows in (b) denote those of period-2. Similarly, we can find the regions of other higher periods. This implies that the present method works by creating a new dynamical system that has γ_i as a system parameter. Choosing one arbitrary point from the shadows of Fig. 2, for example, $\gamma_1=0.3$ and $\gamma_2=-0.3$, we can get the period-1 orbit. The results show in Fig. 3 when the transient process is thrown away. The noncontinuous character of the stabilized flow at the crossing can be clearly appreciated.

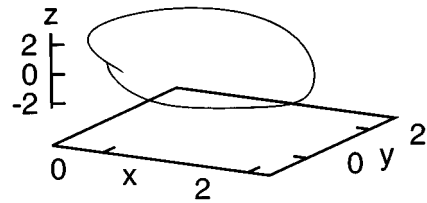


FIG. 3. The stabilized period-1 orbit for additive perturbations method in $\gamma_1=0.3$ and $\gamma_2=-0.3$.

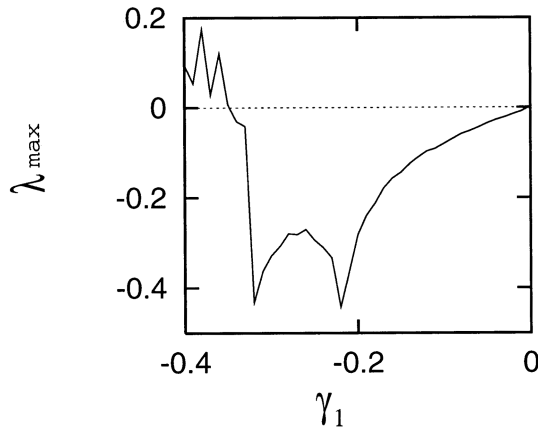


FIG. 4. The relation between the maximum Lyapunov exponent λ_{\max} and the intensity of perturbation γ_1 , where $\gamma_2 = -0.3$.

From Fig. 2 one can see that the shadows do not contain the lines of $\gamma_1 = 0$ or $\gamma_2 = 0$. It means that the periodic orbit cannot be found by only adding periodic pulses on the x variable or y variable of Poincaré section. Our numerical calculation confirms this point. On the other hand, the finite size of shadows in Fig. 2 illustrates that the period-1 or period-2 is stable in some range of γ_1 and γ_2 . In order to confirm this point, we calculate the Lyapunov exponents of Eq. (4). We know that continuous flows necessarily have a zero Lyapunov exponent corresponding to the direction of the flow. Hence, we only need to calculate the maximum Lyapunov exponent for the two-dimensional (2D) Poincaré map. Figure 4 shows the maximum Lyapunov exponent when $\gamma_1 = -0.4 \sim 0$ and $\gamma_2 = -0.3$, where λ_{\max} is negative when γ_1 is in the range of periodic windows for Fig. 2, but positive when γ_1 is out of the range of periodic windows. Thus the new creating periodic orbits are stable (attracting). This is confirmed by using different initial conditions and there is a reasonably large basin of attraction. It implies that the conservative flow becomes dissipative when the periodic pulses is added.

III. MULTIPLICATIVE IMPULSIVE METHOD

The second method is defined by

$$x'_i = x_i(1 + \gamma_i) \quad (5)$$

And the perturbation is applied at the crossing with the Poincaré section, where x_i represents the i th variable of the system, and γ_i defines the strength of the pulse for variable x_i , that can be either positive or negative. In other words, the conservative flow is controlled by changing x_i in such a way that a proportional feedback is applied on the Poincaré section in the form of pulses. The idea is how to choose suitable values of the γ_i so that the system becomes periodic and the regular orbits are approximate to those of the original system. This method has some difference from Ref. [11] where an arbitrary time scale for the perturbations is introduced.

Making the same Poincaré section and the same initial point with the method in Sec. II, we can write Eq. (2) as follows:

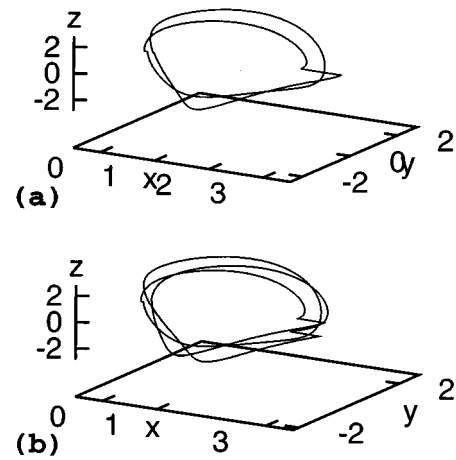


FIG. 5. (a) The stabilized period-2 orbit for multiplicative perturbation method in $\gamma = 0.3$; (b) the stabilized period-3 orbit for multiplicative perturbation method in $\gamma = 0.2$.

$$\begin{aligned} \dot{x} &= y + \gamma x \delta(z) \dot{z} \theta(\dot{z}), \\ \dot{y} &= -x + yz, \\ \dot{z} &= 1 - y^2, \end{aligned} \quad (6)$$

where the meaning of γ , δ , and θ are just the same as that of Eq. (4). Different from Sec. II, we only applied periodic pulses to the x variable. Our numerical calculation shows that it is the same when only periodic pulses are applied to the y variable. Now we let γ vary from -1.0 to 1.0 . We get some periodic windows, for example, a period-1 window when $\gamma = -1.0 \sim -0.4$, a period-3 window when $\gamma = 0.08 \sim 0.20$, a period-2 window when $\gamma = 0.21 \sim 0.52$, a period-1 window when $\gamma = 0.53 \sim 0.65$, and high-periodic states when $\gamma = 0.06 \sim 0.07$, $0.66 \sim 0.67$, and $0.69 \sim 0.71$. Figure 5 shows two typical periodic orbits. It is evident that the points of the stabilized periodic orbit of the Poincaré section do not belong to the original chaotic set, but are rather somehow shifted. Making the same calculation as in Sec. II, we can get the maximum Lyapunov exponent λ_{\max} for the 2D Poincaré map in this case. Figure 6 is the result when $\gamma = 0 \sim 0.70$, where λ_{\max} is negative when γ is in the periodic

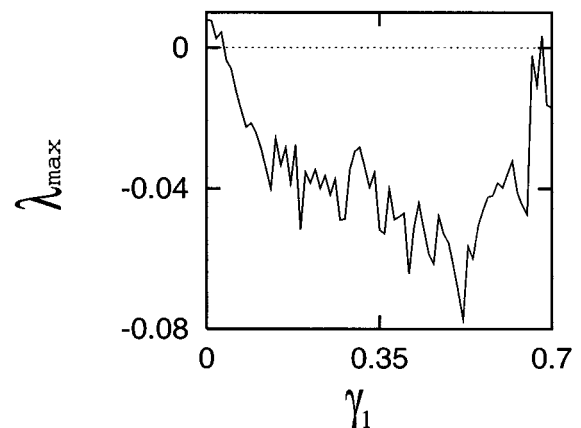


FIG. 6. The relation between the maximum Lyapunov exponent λ_{\max} and the intensity of perturbation γ .

windows and high-periodic states, but positive when γ is out of the range. It illustrates that the new creating periodic orbit is stable.

IV. EFFECTS OF NOISE AND CONCLUSION

In order that it can be effectively considered that a given chaos suppression is useful, having in mind practical applications, one must first check whether the method is robust against the presence of several sources of external noise. In this section, we consider the Gaussian white noise ξ having zero mean and a standard deviation equal to one, generated by using the Box-Müller method [15]. We also introduce additive noise in the form,

$$x'_i = x_i + \rho\xi, \quad (7)$$

and multiplicative noise in the form,

$$x'_i = x_i(1 + \rho\xi), \quad (8)$$

where ρ denotes the intensity of external noise. This noise is applied at each Runge-Kutta integration step.

Figure 7(a) shows the result obtained by considering the presence of multiplicative noise for the period-1 in Fig. 3, and Fig. 7(b) shows the result obtained by considering the presence of multiplicative noise for period-2 in Fig. 5(a). For the case of additive noise, it is just the same. Comparing Fig. 7(a) with Fig. 3, and Fig. 7(b) with Fig. 5(a) without noise, respectively, we can see that the orbits having noise become rough, but they remain within a small region surrounding the noise-free orbit and do not wander over the x - y plane. So they are still periodic. This shows that the periodic impulsive method is robust against weak external noise.

In conclusion, two versions of chaos suppression methods of conservative flow through changes in the system variables have been discussed and applied to case A. Although this method was first presented for the dissipative system [11–13], our results show that it is effective in conservative flow. The methods work by reducing the system dimensionality through a suitably chosen Poincaré cross section of the system, i.e., a plane that is perpendicular to the flow. Two versions of the methods have been implemented, namely, by considering both additive and proportional changes in the

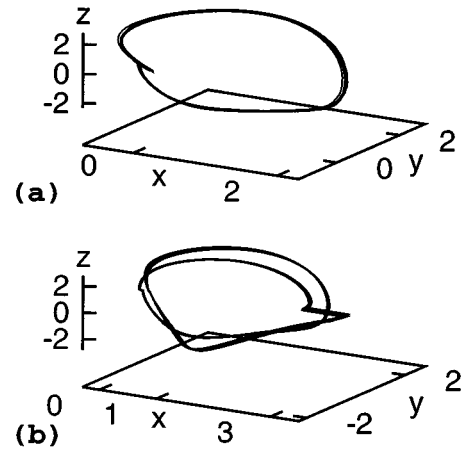


FIG. 7. Effect of noise in the presence of multiplicative noise. (a) The stabilized period-1 orbit for additive impulsive method corresponding to Fig. 3, where the intensity of noise is 1.0×10^{-3} ; (b) the stabilized period-2 orbit for multiplicative impulsive method corresponding to Fig. 5(a), where the intensity of noise is 5.0×10^{-4} .

system variables, where the first is independent of the position of the system on the Poincaré section.

The possibility of choosing different periodic behaviors within these methods has been shown. For the multiplicative impulsive method, the periodic orbit can be controlled by only adding perturbation to one variable, while for the additive impulsive method, the periodic orbit can only be controlled by adding perturbations to two variables at the same time. Furthermore, for producing a stable periodic orbit the intensities of perturbation applied between multiplicative and additive fashion are different. So the results somewhat dependent on the nature of the perturbation. On the other hand, this paper has shown its robustness under the presence of some source of external noise. The negative maximum Lyapunov exponents illustrate that the periodic orbits created by the periodic impulsive methods are stable.

ACKNOWLEDGMENTS

This work was partially supported by the National Natural Science Foundation of China and Science Foundation of China Academy of Engineering Physics.

[1] E. Ott, C. Grebogi, and J. A. Yorke, *Phys. Rev. Lett.* **64**, 1196 (1990).
 [2] Y. Braiman and I. Goldhirsch, *Phys. Rev. Lett.* **66**, 2545 (1991).
 [3] Y. Liu and J. R. R. Leite, *Phys. Lett. A* **185**, 35 (1994).
 [4] E. R. Hunt, *Phys. Rev. Lett.* **67**, 1953 (1991).
 [5] K. Pyragas, *Phys. Lett. A* **170**, 421 (1992).
 [6] E. A. Jackson, *Phys. Lett. A* **151**, 478 (1990).
 [7] E. A. Jackson, *Physica D* **50**, 341 (1991).
 [8] Liu Zonghua and Chen Shigang, *Phys. Rev. E* **55**, 199 (1997).
 [9] Liu Zonghua and Chen Shigang, *Chin. Phys. Lett.* **14**, 85

(1997).
 [10] Y. C. Lai, M. Ding, and C. Grebogi, *Phys. Rev. E* **47**, 86 (1993).
 [11] M. A. Matías and J. Güémez, *Phys. Rev. Lett.* **72**, 1455 (1994).
 [12] M. A. Matías and J. Güémez, *Phys. Rev. E* **54**, 198 (1996).
 [13] J. M. Gutiérrez, A. Iglesias, J. Güémez, and M. A. Matías, *Bif. Chaos* **6**, 1351 (1996).
 [14] J. C. Sprott, *Phys. Rev. E* **50**, R647 (1994).
 [15] W. H. Press, B. P. Flannery, S. A. Teukolsky, and W. T. Vetterling, *Numerical Recipes: The Art of Scientific Computing* (Cambridge University Press, New York, 1986).